

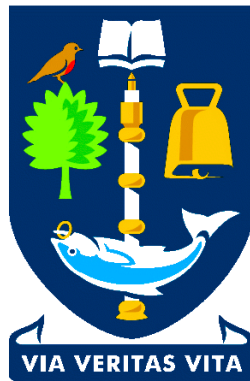
# Heavy Semileptonic Form Factors from Lattice Quantum Chromodynamics

*Euan McLean*

*Supervised by Prof. Christine Davies*

*Submitted in fulfillment of the requirements for the degree of  
Doctor of Philosophy*

*April 2019*



*The University of Glasgow  
College of Science and Engineering*



---

## Heavy Semileptonic Form Factors from Lattice Quantum Chromodynamics

### Abstract:

I did some lattice

---



---

### **Declaration of originality**

This thesis is my own work, except where explicit attribution to others is made. In particular Chapters ... are based on the following publications:

All results and figures presented in these chapters are my own, except for ...

---



*please help i am trapped in this computer*





## Acknowledgments

I claim sole credit for everything in this thesis.



# Contents

<b>1</b>	<b>Background and Motivation</b>	<b>1</b>
1.1	Testing the Standard Model . . . . .	1
1.2	Flavour Physics . . . . .	1
1.2.1	The CKM Matrix . . . . .	1
1.2.2	Weak Decays . . . . .	1
1.2.3	Flavour Anomalies . . . . .	4
1.2.4	Lepton Flavour Violation . . . . .	4
<b>2</b>	<b>Heavy Semileptonic Decays</b>	<b>7</b>
2.1	Strong Interaction Physics . . . . .	7
2.1.1	Quantum Chromodynamics . . . . .	7
2.1.2	Chiral Perturbation Theory . . . . .	7
2.2	Heavy Quark Physics . . . . .	7
2.2.1	HQET . . . . .	7
2.2.2	NRQCD . . . . .	7
2.3	Form Factors . . . . .	7
2.3.1	Analyticity . . . . .	8
2.3.2	$z$ -Expansion . . . . .	8
2.4	Renormalization of Currents . . . . .	8
<b>3</b>	<b>Lattice Quantum Chromodynamics</b>	<b>11</b>
3.1	Lattice Gauge Fields . . . . .	12
3.1.1	The Wilson Gauge Action . . . . .	12
3.1.2	Improvements . . . . .	12
3.2	Lattice Fermions . . . . .	12
3.2.1	The Doubling Problem . . . . .	12
3.2.2	Staggered Quarks . . . . .	14
3.2.3	Highly Improved Staggered Quarks . . . . .	15
<b>4</b>	<b>Lattice Calculations</b>	<b>19</b>
4.1	Correlation Functions from Lattice Simulations . . . . .	19
4.1.1	Path Integral . . . . .	20
4.1.2	Dirac Operator Inversion . . . . .	20

4.1.3	Random Wall Sources . . . . .	20
4.2	Analysis of Correlation Functions . . . . .	23
4.2.1	Non-Linear Regression . . . . .	23
4.2.2	Signal/Noise Ratio . . . . .	27
4.3	Dealing with Heavy Quarks . . . . .	29
4.3.1	Heavy HISQ . . . . .	29
4.3.2	Lattice NRQCD . . . . .	29
4.4	Renormalization of Currents . . . . .	29
4.4.1	Non-perturbative Renormalization of HISQ Currents . . . . .	30
4.4.2	Matching NRQCD currents to $\overline{MS}$ . . . . .	30

# Background and Motivation

---

## 1.1 Testing the Standard Model

## 1.2 Flavour Physics

### 1.2.1 The CKM Matrix

### 1.2.2 Weak Decays

The key motivations for studying decays like the  $B_s \rightarrow D_s l \nu$  are:

- Determination of CKM matrix elements. Specifically, by combining the theoretical prediction and an observed branching fraction of  $B_s \rightarrow D_s l \nu$ ,  $|V_{cb}|$  can be extracted.
- Precision tests of the standard model. There are currently a number of tensions between experiment and the standard model predictions of  $B$  decays, some closely related to  $B_s \rightarrow D_s l \nu$  [28].

We will first discuss the general ideas in computing semileptonic decays.

Semileptonic decays are useful for studying the sector of the standard model (SM) which couples quarks to the weak force [31]:

$$\mathcal{L}_W = \frac{g}{\sqrt{2}} \left[ V_{ij} J_{ij}^\mu W_\mu^+ + V_{ij}^\dagger J_{ij}^{\mu\dagger} W_\mu^- \right] \quad (1.1)$$

$J_\mu^{ij} = \bar{u}_i \gamma_\mu \frac{1}{2} (1 - \gamma_5) d_j$  are the weak currents,  $\underline{u} = (u, c, t)$  and

$\underline{d} = (d, s, b)$  are the quark fields,  $g$  is the weak coupling constant,  $W^\pm$  are the charged weak bosons, and  $V$  is the (unitary) Cabibbo-Kobayashi-Maskawa (CKM) matrix.  $V_{ij}$  can be thought of as a matrix of couplings which dictate the probability

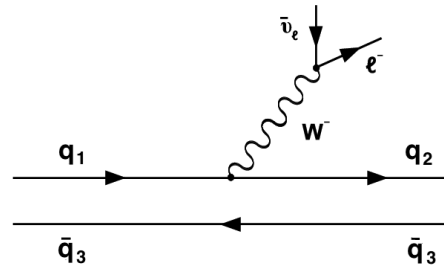


Figure 1.1: Semileptonic decay at tree level

of mixing between two quark flavours, for example the amplitude of a  $b$  decaying to a  $u$  (and emitting a  $W$ ) is proportional to  $V_{13} \equiv V_{ub}$ .

A semileptonic decay is any *hardon*  $\rightarrow$  *hadron* + *leptons* process. Fig. 1.2 shows the tree level (in weak coupling) contribution to a semileptonic decay. We denote a meson with valence quark content  $q$  and  $q'$  as  $M_{qq'}$ . The  $M_{q_1\bar{q}_3} \rightarrow M_{q_2\bar{q}_3} l\bar{\nu}_l$  decay ( $l$  is some charged lepton and  $\bar{\nu}_l$  is it's neutrino) is proportional to  $V_{q_1q_2}$  at tree level.

This is given by

$$\mathcal{M} = \left(\frac{ig}{\sqrt{2}}\right)^2 V_{q_1q_2} \langle M_{q_2\bar{q}_3}, l\bar{\nu} | J_\alpha^{q_1\bar{q}_2} D_W^{\alpha\beta}(p^2) J_\beta^{l\bar{\nu}} | M_{q_1\bar{q}_3} \rangle \quad (1.2)$$

$J^{l\bar{\nu}}$  is the analog of the quark currents  $J^{q_1\bar{q}_2}$ , since the  $W$  couples in the same way to leptons (with  $V$  replaced by a unit matrix). If the external momenta of the process  $p^2$  are much smaller than the  $W$  mass, one can remove the  $W$  propagator from the tree level amplitude [6];

$$\left(\frac{ig}{\sqrt{2}}\right)^2 D_W^{\mu\nu}(p^2) = \left(\frac{ig}{\sqrt{2}}\right)^2 \left(\frac{-ig^{\mu\nu}}{p^2 - M_W^2}\right) = \underbrace{\frac{i}{M_W^2} \left(\frac{ig}{\sqrt{2}}\right)^2}_{\equiv -2\sqrt{2}G_F} g^{\mu\nu} + \mathcal{O}\left(\frac{p^2}{M_W^4}\right) \quad (1.3)$$

Then  $\mathcal{M}$  can be factorised;

$$\begin{aligned} \mathcal{M} &\simeq -2\sqrt{2}G_F V_{q_1q_2} \langle M_{q_1\bar{q}_3}, l\bar{\nu} | J_\mu^{q_1\bar{q}_2} J^{l\bar{\nu}\mu} | M_{q_2\bar{q}_3} \rangle \\ &= -2\sqrt{2}G_F V_{q_1q_2} \langle l\bar{\nu} | J^{l\bar{\nu}\mu} | 0 \rangle \langle M_{q_1\bar{q}_3} | J_\mu^{q_1\bar{q}_2} | M_{q_2\bar{q}_2} \rangle \\ &\equiv -2\sqrt{2}V_{q_1q_2} G_F L^\mu H_\mu. \end{aligned} \quad (1.4)$$

$L_\mu$  can be computed in perturbation theory. The hadronic matrix element  $H_\mu$  however, due to the non-perturbative nature of QCD at low energies, cannot be computed analytically. It is quantities such as  $H_\mu$  that we wish to calculate in lattice QCD.

Speaking heuristically, if one can calculate the quantity  $G_F L^\mu H_\mu$  from theory, and measures the amplitude of the process  $\mathcal{M}$ , they could then rearrange equation (1.4) to deduce  $V_{q_1q_2}$ . Speaking more practically, the relevant equation is, for example, for the  $B_s \rightarrow D_s l\nu$  decay [28]:

$$\frac{d\Gamma}{dq^2} = \eta_{EW} \frac{G_F^2 |V_{cb}|^2}{24\pi^3 M_{B_s}^2} \left(1 - \frac{m_l^2}{q^2}\right)^2 |\underline{p}| \quad (1.5)$$

$$\times \left[ \left(1 + \frac{m_l^2}{2q^2}\right) M_{B_s}^2 |\underline{p}| f_+^2(q^2) + \frac{3m_l^2}{8q^2} (M_{B_s}^2 - M_{D_s}^2)^2 f_0^2(q^2) \right] \quad (1.6)$$

where  $m_l$  is the mass of the charged lepton,  $\eta_{EW}$  is an electroweak correction factor,  $q^2$  is the momentum transfer,  $d\Gamma/dq^2$  is the branching fraction, and  $f_{0,+}(q^2)$  are the form factors associated with the decay, to be defined in ???. Given experimental data for  $d\Gamma/dq^2$  and theoretical data for  $f_{0,+}(q^2)$ , one can deduce  $|V_{cb}|$ .

What is the value of determining CKM elements? Firstly, uncertainty in CKM elements are the dominant error in many standard model predictions.  $V$  elements can also test the standard model.  $V$  is unitary by definition. However, if there were more than 3 generations of quark, requiring  $V$  to be 4x4 or larger, the 3x3 submatrix which couples the 3 known generations would not itself be unitary in general ([32] ch. 29). Therefore, if one can deduce the elements of the 3x3  $V$  to high enough precision to show it is not unitary, this would be indirect evidence for new physics.

Unitarity imposes a constraint on each row of  $V$ . The current status of the unitarity of  $V$  can be read off from below (each quantity should be zero for unitarity to hold) [3]:

$$\begin{aligned} |V_{ud}|^2 + |V_{us}|^2 + |V_{ub}|^2 - 1 &= -0.020(9) \\ |V_{cd}|^2 + |V_{cs}|^2 + |V_{cb}|^2 - 1 &= 0.06(3) \end{aligned} \quad (1.7)$$

both of the above relations display a  $\sim 2\sigma$  deviation from unitarity. More precise values of these parameters are needed to discover if CKM is infact non-unitary.

Now we consider  $|V_{cb}|$  specifically.  $|V_{cb}|$  is the dominant uncertainty in many standard model predictions of rare decays, such as  $B_s \rightarrow \mu^+ \mu^-$ ,  $K \rightarrow \pi \nu \bar{\nu}$ , and the CP violation parameter  $\epsilon_K$  [28]. The FLAG working group quotes their average  $|V_{cb}|$  to currently be [3]:

$$|V_{cb}| = 0.04085(95) \quad (1.8)$$

However, the water is slightly muddled by the presence of tensions between different determinations of  $|V_{cb}|$ , namely between that deduced from studying  $B \rightarrow D^* l \nu$ , and an inclusive analysis of  $B \rightarrow X_c l \nu$  where  $X_c$  is any meson containing a  $c$  quark [28]:

$$|V_{cb}|_{\text{inclusive}} = 0.04221(78) , |V_{cb}|^{B \rightarrow D^* l \nu} = 0.03904(49)_{\text{expt.}}(53)_{\text{QCD}}(19)_{\text{QED}} \quad (1.9)$$

A recent review of  $|V_{cb}|$  determinations from the lattice is given in [33]. This issue would benefit from a  $|V_{cb}|$  determination from another channel, like  $B_s \rightarrow D_s l \nu$ ,

to flesh out the landscape of  $|V_{cb}|$  values and pinpoint the source of the tension, if there is any.

### 1.2.3 Flavour Anomalies

There are a number of tensions currently between theory and experiment in  $B$  decays, whose true nature can be elucidated by our  $B_s \rightarrow D_s l \nu$  study, and eventual  $B \rightarrow D l \nu$  study.

Define the ratios

$$R(X) = \frac{\mathcal{B}(B \rightarrow X \tau \nu_\tau)}{\mathcal{B}(B \rightarrow X l \nu_l)} \quad (1.10)$$

where  $l = e$  or  $\mu$ . These can be computed either purely from a lattice calculation, or purely from experimental data, independently of the associated CKM element. It therefore can be used for comparison between experiment and the standard model.  $R(D^*)$  contains a  $2.1\sigma$  discrepancy [1]:

$$R(D^*)|_{\text{SM}} = 0.252(3) , R(D^*)|_{\text{LHCb}} = 0.336(27)_{\text{sys}}(30)_{\text{stat}} \quad (1.11)$$

The issue is similarly present for  $R(D)$  [26]:

$$R(D)|_{\text{SM}} = 0.299(7) , R(D)|_{\text{exp}} = 0.391(28)_{\text{sys}}(41)_{\text{stat}} \quad (1.12)$$

where in this case  $R(D)|_{\text{expt}}$  is a world average of experimental values. Our eventual study of  $B \rightarrow D l \nu$  will produce a new standard model determination of  $R(D)$ , helping shed light on the issue.

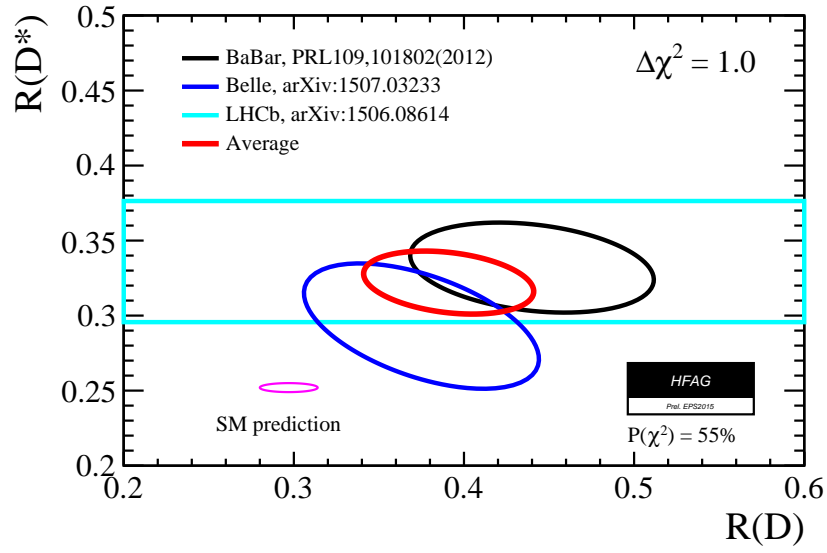
Besides these, there are also tensions in the quantities [2]:

$$R'(K^{(*)}) = \frac{\mathcal{B}(B \rightarrow K^{(*)} \mu^+ \mu^-)}{\mathcal{B}(B \rightarrow K^{(*)} e^+ e^-)} \quad (1.13)$$

All of the above anomalies are suggestive of lepton flavour violating effects. Various BSM models have been suggested; hot topics include Leptoquarks,  $Z'$  models, and partial compositeness [2].

### 1.2.4 Lepton Flavour Violation



Figure 1.2:  $R(D)/R(D^*)$  determinations from standard model and experiment [18]



# Heavy Semileptonic Decays

---

## 2.1 Strong Interaction Physics

### 2.1.1 Quantum Chromodynamics

### 2.1.2 Chiral Perturbation Theory

## 2.2 Heavy Quark Physics

### 2.2.1 HQET

### 2.2.2 NRQCD

## 2.3 Form Factors

We now turn to some more technical details about semileptonic decays.

We will refer to the 4-momenta and mass of the initial and final states as  $p_{1,2}, M_{1,2}$  respectively, and define the 4-momentum taken away by the  $W^\pm$  boson as  $q \equiv p_2 - p_1$ . We work in the rest frame of the initial meson, in which

$$q^2 = M_1^2 + M_2^2 - 2M_1 E_2. \quad (2.1)$$

There is a physically allowed range of values for an on-shell  $q^2$ . The minimum is when all of the 3-momentum of the initial state is taken by the final meson,  $q_{\min}^2 = 0$ .  $q^2$  is maximised when all of the 3-momentum is taken by the boson,  $\underline{p}_2^2 = 0 \rightarrow E_2 = \sqrt{M_2^2 + \underline{p}_2^2} = M_2 \rightarrow q_{\max}^2 = M_1^2 - M_2^2 - 2M_1 M_2 = (M_2 - M_1)^2$ . So

$$0 \leq q^2 \leq (M_2 - M_1)^2 \quad (2.2)$$

This also creates an allowed range for the final meson 3-momentum:

$$0 < \underline{p}_2^2 < \left( \frac{M_1^2 + M_2^2}{2M_1} \right)^2 - M_2^2 \quad (2.3)$$

Hadronic matrix elements like  $H_\mu$  from sec. ?? can be parameterised in terms of form factors. The current operator between the states is a conserved current, so then the matrix element must be proportional to only conserved quantities, namely, elements of the stress-energy tensor. Lorentz invariance requires indices on either side of such a relation match, so a matrix element with a single Lorentz index can only be proportional to 4-momenta.

Let us consider the case where the two states in the matrix element are pseudoscalar mesons (as in  $B_s \rightarrow D_s l \nu$ ), with an insertion of a left-handed current (i.e. the coupling to the  $W^\pm$  in (1.1)),  $J_\mu^{ij} = \bar{u}_i \gamma_\mu \frac{1}{2}(1 - \gamma_5) d_j$ . This can be written as  $J_\mu^{ij} = V_\mu^{ij} - A_\mu^{ij}$ , these are the vector and axial vector currents.

The axial vector evaluated between two pseudoscalar states must vanish because the combination is not parity invariant thus does not contribute in pure QCD, leaving just the vector current. The most common parameterisation is:

$$\langle P_2(p_2) | V^\mu | P_1(p_1) \rangle = f_+(q^2) \left[ p_1^\mu + p_2^\mu - \frac{M_1^2 - M_2^2}{q^2} q^\mu \right] + f_0(q^2) \frac{M_1^2 - M_2^2}{q^2} q^\mu \quad (2.4)$$

Where  $|P_i(p_i)\rangle$  is a pseudoscalar meson state with momentum  $p_i$ .

### 2.3.1 Analyticity

### 2.3.2 z-Expansion

## 2.4 Renormalization of Currents

The currents  $V_\mu$  and  $A_\mu$  are conserved in the Chiral limit (quark masses  $\rightarrow 0$ ). This can be shown via Noether's theorem: consider a theory containing a number of fields  $\{\varphi_i\}$ , which transform under a group  $G$  by

$$\varphi_i \rightarrow \varphi_i(x) - i\epsilon_a(x) F_{i,a}[\{\varphi\}] \quad (2.5)$$

It can be shown that there exists currents

$$J_a^\mu = -i \frac{\partial \mathcal{L}}{\partial \partial_\mu \varphi_i} F_{i,a} \quad (2.6)$$

which obey

$$J_a^\mu = \frac{\partial \delta \mathcal{L}}{\partial \partial_\mu \epsilon_a} \quad (2.7)$$

$$\partial_\mu J_a^\mu = \frac{\partial \delta \mathcal{L}}{\delta \epsilon_a} \quad (2.8)$$

where  $\delta \mathcal{L}$  is the result of an infinitesimal  $G$  operation, i.e.  $G : \mathcal{L} \rightarrow \mathcal{L} + \delta \mathcal{L}$ . From (2.8), we see that if the theory is symmetric under the generator parameterised by  $\epsilon_a$ , then  $J_a^\mu$  is a conserved current.

In the chiral limit, QCD with  $N$  flavors has the accidental global symmetry ("chiral symmetry")  $U(N)_L \times U(N)_R$ :

$$q_{L/R} \rightarrow \exp(-i\theta_a^{L/R} \lambda_a) q_{L/R} \quad (2.9)$$

where  $q$  is a vector in flavor space, and  $\lambda_a$  are the generators of  $U(N)$  in the fundamental representation and acts on flavor. Applying (2.7) and (2.8) to QCD we get the conserved currents:

$$J_{L/R}^{\mu,a} = \bar{q}_{L/R} \gamma^\mu \lambda_a q_{L/R} \quad (2.10)$$

$$\partial_\mu J_{L/R}^{\mu,a} = 0 \quad (2.11)$$

$J_{L/R}$  are often expressed instead in terms of *vector* and *axial* currents

$$V^{\mu,a} = J_L^{\mu,a} + J_R^{\mu,a} = \bar{q} \gamma^\mu \lambda_a q \quad (2.12)$$

$$A^{\mu,a} = J_L^{\mu,a} - J_R^{\mu,a} = \bar{q} \gamma^\mu \gamma_5 \lambda_a q \quad (2.13)$$

which are conserved currents corresponding to the vector and axial symmetries  $U(N)_V$  and  $U(N)_A$ , consisting of simultaneous  $L/R$  transformations above with constraints  $\theta_a^L = \pm \theta_a^R$ . Vector and axial currents between any two individual flavours, i.e.

$$V_{ij}^\mu = \bar{q}_i \gamma^\mu q_j \quad (2.14)$$

$$A_{ij}^\mu = \bar{q}_i \gamma^\mu \gamma_5 q_j \quad (2.15)$$

are also conserved, since they can be constructed from linear combinations of  $V^{\mu,a}$  and  $A^{\mu,a}$ .

$U(N)$  can be broken up into  $SU(N) \times U(1)$ , where  $U(1)$  is a singlet transformation, i.e., of the form of (2.9) with  $\lambda = 1$ . When QCD is quantized, it

develops an anomaly which breaks the singlet axial symmetry. This reduces the symmetry group to  $SU(N)_V \times SU(N)_A \times U(1)_V$ , and prevents the corresponding axial singlet current  $A^{\mu,0}$  from being conserved.

In the case of non-zero quark mass, the chiral symmetry is broken. This leads to (2.8) for the vector and axial currents evaluating instead as

$$\partial_\mu V^{\mu,a} = i\bar{q}[M, \lambda_a]q \quad (2.16)$$

$$\partial_\mu A^{\mu,a} = i\bar{q}\{M, \lambda_a\}q \quad (2.17)$$

where  $M$  is the quark mass matrix in flavor space. These are the partially conserved axial and vector current identities (PCAC and PCVC). By taking a linear combination of these equations, one can derive PCAC and PCVC for individual flavors:

$$\partial_\mu V_{ij}^\mu = i(m_i - m_j)\bar{q}_i q_j \equiv i(m_i - m_j)S_{ab} \quad (2.18)$$

$$\partial_\mu A_{ij}^\mu = i(m_i - m_j)\bar{q}_i \gamma_5 q_j \equiv i(m_i - m_j)P_{ij} \quad (2.19)$$

We refer to  $S$  as the scalar current and  $P$  as the pseudoscalar. These identities translates straightforwardly to expectation values:

$$(p_1 - p_2)_\mu \langle \psi(p_2) | V_{ij}^\mu | \phi(p_1) \rangle = (m_i - m_j) \langle \psi(p_2) | S_{ij} | \phi(p_1) \rangle \quad (2.20)$$

$$(p_1 - p_2)_\mu \langle \psi(p_2) | A_{ij}^\mu | \phi(p_1) \rangle = (m_i - m_j) \langle \psi(p_2) | P_{ij} | \phi(p_1) \rangle \quad (2.21)$$

where  $|\psi(p)\rangle$  and  $|\phi(p)\rangle$  are arbitrary states containing momentum  $p$ .

These are powerful tools for connecting expectation values of different currents. For example, by combining (2.20) and (2.4), we see that:

$$\langle P_2(p_2) | S_{ij} | P_1(p_1) \rangle = \frac{M_1^2 - M_2^2}{m_i - m_j} f_0(q^2) \quad (2.22)$$

Hence we have an extra route to accessing  $f_0$ . In a lattice simulation which computes expectation values of  $V^\mu$ , one could constrain  $f_0$  by also computing the scalar current on the lattice, then use the rest of the information in  $V^\mu$  to constrain  $f_+$ .

# Lattice Quantum Chromodynamics

---

At low energies ( $\sim 200\text{MeV}$  and below), QCD becomes non-perturbative, in other words, the coupling  $\alpha_s$  becomes  $\mathcal{O}(1)$ , and an expansion in  $\alpha_s$  (as in perturbation theory) will not be dominated by the leading orders [32]. We require an alternative.

The expectation value of an observable  $\mathcal{O}$  in a Yang-Mills theory can be expressed as a Euclidean path integral [22];

$$\langle \mathcal{O} \rangle = \int \mathcal{D}A \mathcal{D}\psi \mathcal{D}\bar{\psi} \mathcal{O} e^{-S[A, \psi, \bar{\psi}]}, \quad (3.1)$$

where  $A$  is a gauge field,  $\psi(\bar{\psi})$  is an (anti)fermion field,  $S$  is the Euclideanised classical action, and  $\mathcal{D}$  denotes integration over all configurations of a field. "Euclideanised" refers to a Wick rotation  $t \rightarrow it$  in  $S$ . In the perturbative approach, we would expand  $\exp(-\text{interacting part of } S)$  resulting in a power series in the gauge coupling populated by Feynman diagrams.

The other option is to instead carry out the integral directly. This can only be done numerically. Since it's not numerically feasible to carry out an infinite number of integrals, one must approximate spacetime as a discrete 4 dimensional lattice with spacing " $a$ " between lattice sites, finite spacial volume  $L_x^3$  and finite temporal extent  $L_t$ . The functional integral becomes

$$\int \mathcal{D}A \mathcal{D}\psi \mathcal{D}\bar{\psi} = \prod_n \int dU(x_n) d\psi(x_n) d\bar{\psi}(x_n), \quad (3.2)$$

where  $n$  is a 4-vector with integer components labelling the sites, and  $x_n^\mu = an^\mu$ . This has a second benefit which is to naturally regularize the theory with a momentum cutoff  $\Lambda \sim 1/a$  [22]. The gauge field has been replaced with the gauge "link":

$$U_\mu(x) \equiv \exp \left( i g a A_\mu \left( x + \frac{a\hat{\mu}}{2} \right) \right) \in SU(N_c), \quad (3.3)$$

$g$  is the gauge coupling,  $\hat{\mu}$  is a unit vector in the  $\mu$  direction. Parameterizing the gauge fields this way is motivated by the geometrical interpretation of Yang-Mills theories on discrete spacetime and the requirement of exact gauge symmetry [27].

## 3.1 Lattice Gauge Fields

### 3.1.1 The Wilson Gauge Action

#### 3.1.2 Improvements

## 3.2 Lattice Fermions

The interacting Dirac action is most naively discretised with

$$S_F = \sum_{x,\mu} \bar{\psi}(x) \gamma_\mu \nabla_\mu \psi(x) + m \sum_x \bar{\psi}(x) \psi(x), \quad (3.4)$$

where  $\nabla_\mu$  is the gauge covariant finite difference operator,

$$\nabla_\mu \psi(x) = \frac{1}{2a} (U_\mu(x) \psi(x + a\hat{\mu}) - U_\mu^\dagger(x - a\hat{\mu}) \psi(x - a\hat{\mu})). \quad (3.5)$$

In appendix ?? we describe the doubling problem. This is the observation that the propagator for a fermion obeying (3.7),  $M^{-1}(k)$  has the property

$$M^{-1}(k + \frac{\pi}{a}\zeta) = \gamma_{5\mu} M^{-1}(k) \gamma_{5\mu} \quad (3.6)$$

For 16 4-vectors  $\zeta_\mu \in \mathbb{Z}_2$ . This leads to 16 poles in the fermion spectrum, therefore 16 distinct excitations (called *tastes*). We require a way of removing the 15 unphysical excitations.

### 3.2.1 The Doubling Problem

The interacting Dirac action is most naively discretised with

$$S_F = \sum_{x,\mu} \bar{\psi}(x) \gamma_\mu \nabla_\mu \psi(x) + m \sum_x \bar{\psi}(x) \psi(x), \quad (3.7)$$

where  $\nabla_\mu$  is the gauge covariant finite difference operator,

$$\nabla_\mu \psi(x) = \frac{1}{2a} (U_\mu(x) \psi(x + a\hat{\mu}) - U_\mu^\dagger(x - a\hat{\mu}) \psi(x - a\hat{\mu})). \quad (3.8)$$



An issue arises with fermions on the lattice, known as the doubling problem.  $S_F$  is invariant under a so-called "doubling symmetry", which is generated by

$$\psi(x) \rightarrow \mathcal{B}_\mu \psi(x) \equiv (-1)^{x_\mu/a} \gamma_{5\mu} \psi(x) \quad (3.9)$$

$$\bar{\psi}(x) \rightarrow \bar{\psi}(x) \mathcal{B}_\mu^\dagger \equiv (-1)^{x_\mu/a} \bar{\psi}(x) \gamma_{5\mu}^\dagger \quad (3.10)$$

where  $\gamma_{5\mu} = i\gamma_\mu \gamma_5$ . The product space of these form a group of 16 elements  $\{\mathcal{B}_\zeta\}$ , labeled by vectors  $\zeta$  with  $\zeta_\mu \in \mathbb{Z}_2$  (e.g. the element  $\mathcal{B}_0 \mathcal{B}_1$  is labeled by  $\zeta = (1, 1, 0, 0)$ ).

The physical signifiacnce of this symmetry can be seen when we study it's effect on the action. First, notice that

$$\mathcal{B}_\mu \psi(x) = \gamma_{5\mu} \sum_k \tilde{\psi}(k) e^{i(k + \frac{\pi}{a}\hat{\mu}) \cdot x} \quad (3.11)$$

$$= \gamma_{5\mu} \sum_k \tilde{\psi}(k - \frac{\pi}{a}\hat{\mu}) e^{ik \cdot x} \quad (3.12)$$

where  $k$  is a set of discrete 4-momenta. The action in momentum space can be written as

$$S = \sum_k \tilde{\bar{\psi}}(k) M(k) \tilde{\psi}(k) \quad (3.13)$$

after the operation of  $\mathcal{B}_\mu$  it becomes

$$S \rightarrow \sum_k \tilde{\bar{\psi}}(x)(k) \gamma_{5\mu} M(k + \frac{\pi}{a}\hat{\mu}) \gamma_{5\mu} \tilde{\psi}(k) \quad (3.14)$$

Since we know  $S$  is invariant under this transformation, it must be true that  $\gamma_{5\mu} M(k + \frac{\pi}{a}\hat{\mu}) \gamma_{5\mu} = M(k)$ , and therefore

$$M^{-1}(k + \frac{\pi}{a}\hat{\mu}) = \gamma_{5\mu} M^{-1}(k) \gamma_{5\mu} \quad (3.15)$$

$M^{-1}$  is the propagator for the fermion field, so 3.15 shows that the spectrum of the fermion is periodic, with a period of  $\pi/a$ . We expect a pole in  $M^{-1}(k)$  where  $k \sim m$ , where  $m$  is the pole mass of the fermion, but there will now be a second pole at  $m + \pi/a$ . This will be around the natural cutoff imposed by the lattice  $1/a$ , and any higher poles like  $m + 2\pi/a$  is far above the cutoff so will not contribute.

Generalizing this argument to all elements of the doubling symmetry, we see that

$$M^{-1}(k + \frac{\pi}{a}\zeta) = \gamma_{5\mu} M^{-1}(k) \gamma_{5\mu} \quad (3.16)$$

leading to 16 poles in the fermion spectrum, therefore 16 distinct excitations (called *tastes*).

We now show that there are only 4 tastes in the staggered quark formalism. One can isolate a single taste by a block-scaling procedure:

$$\psi^{(\zeta)}(x_B) = \sum_{\delta x_\mu \in \mathbb{Z}_2} \mathcal{B}_\zeta \psi(x_B + \delta x) \quad (3.17)$$

For example, for  $\zeta = 0$ , it would only contain the original non-doubler taste, since all other poles at  $|k| \sim \psi/a$  have been integrated out. For  $\zeta \neq 0$ , the  $\mathcal{B}_\zeta$  operator pushes the  $\zeta$  doubler to where the  $\zeta = 0$  taste originally was in  $k$  space, then the blocking procedure integrates out the rest. Now writing this isolated taste in terms of  $\chi$  we arrive at:

$$\psi^{(\zeta)}(x_B) = \sum_{\delta x_\mu \in \mathbb{Z}_2} \Omega(\delta x) \mathcal{B}_\zeta(0) \chi(x + \delta x) \quad (3.18)$$

Recall we set  $\chi(x) = (\chi_1(x), 0, 0, 0)$ . The product  $\Omega(\delta x) \mathcal{B}_\zeta(0)$  is simply a product of gamma matrices, so can only serve to "scramble" the elements of  $\chi$ . Then, in the staggered formalism, all 16 tastes  $\psi^{(\zeta)}$  amount to only 4 distinguishable fermions:  $(\chi_1, 0, 0, 0)$ ,  $(0, \chi_1, 0, 0)$ ,  $(0, 0, \chi_1, 0)$ ,  $(0, 0, 0, \chi_1)$  (with factors of  $(-1)$  and  $i$ ).

### 3.2.2 Staggered Quarks

There are a number of solutions to this problem. The most straightforward is to modify the action to push the mass of the unwanted tastes above the momentum cutoff, preventing it from effecting the dynamics ("*Wilson fermions*") ([11] ch.6.2). However, actions of this type explicitly break Chiral symmetry. Among other issues, this causes additive renormalization of the fermion mass, immensely complicating the renormalization procedure.

Another approach, known as *staggered quarks* ([11] ch.6.3), partially resolves the doubling issue while retaining chiral symmetry. This is the method we use in our study. Other notable approaches besides Wilson and staggered quarks include *domain wall* [21] and *overlap* [29] fermions.

The general idea of staggered fermions is the following. Redefine the fields

according to

$$\psi(x) = \prod_{\mu} (\gamma_{\mu})^{x_{\mu}/a} \chi(x) \equiv \Omega(x) \chi(x) \quad (3.19)$$

In terms of the new spinor variables  $\chi(x)$ , the naive action (3.7) becomes

$$S_F = \bar{\chi}(x) [\alpha_{\mu}(x) \nabla_{\mu} + m] \chi(x) \quad (3.20)$$

where  $\alpha_{\mu}(x) = (-1)^{\sum_{\nu < \mu} x_{\nu}/a}$ . The action is now diagonal in spin, leading to 4 decoupled grassman variables with identicle actions and identicle coupling to the gauge field. As a result,  $\chi$  propagators (on fixed gauge backgrounds) are spin diagonal:

$$M_{\chi}^{-1}(x, y)[U] = s(x, y)[U] \mathbf{1}_{\text{spin}} \quad (3.21)$$

One need only to include a single component of  $\chi$  in a simulation (i.e. fix  $\chi = (\chi_1, 0, 0, 0)$ ). Then they can compute  $M_{\chi}^{-1}(x, y)[U]$  to obtain  $s(x, y)$ . Then, using the inverse of (3.19),  $s(x, y)$  can be transformed to a propagator of the original spinors:

$$M_{\psi}^{-1}(x, y)[U] = s(x, y)[U] \Omega(x) \Omega^{\dagger}(y) \quad (3.22)$$

This is clearly computationally beneficial. But also, by shaving off the other spinor components, one reduces the number propagating degrees of freedom by a factor of 4. This cuts the number of tastes from 16 down to 4 (this is shown in appendix ??).

The remaining multiplicity is tacked in 3 steps:

1. Ensure only one taste is created and destroyed in the propagator.
2. Minimize the interaction between tastes by modifying the action.
3. Remove contributions of extra tastes in the sea by taking  $\det M \rightarrow \sqrt[4]{\det M}$  in (4.3).

Step 3 can be justified by the following - in the  $a \rightarrow 0$  limit,  $\det M$  tends to  $(\det M^{(0)})^4$ , where  $M^{(0)}$  is the Dirac operator for a single taste. Then, taking the 4th root (in principle) reduces the determinant to that of a sea containing 1 taste.

### 3.2.3 Highly Improved Staggered Quarks

Step 2 above is the guiding principle for the action we use in our study, the Highly Improved Staggered Quark action (HISQ).

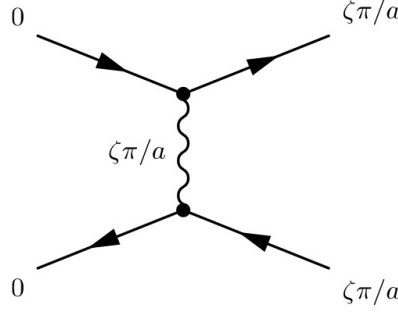


Figure 3.1: Taste mixing at tree level.

Interaction between different tastes ("taste mixing") is dominated by the process in fig. 3.1. In HISQ, this is suppressed by modifying the gauge fields in such a way as to minimize the coupling between a gluon with momentum  $\pi/a$  and the fermions, in other words, minimize the vertices in fig. 3.1. To this end, one can change the action so that fermions only couple to *smeared* gauge links, in which high frequency excitations have been removed.

Define the first and second covariant derivative operators:

$$\begin{aligned} \delta_\rho U_\mu(x) &\equiv \frac{1}{a} (U_\rho(x) U_\mu(x + a\hat{\rho}) U_\rho^\dagger(x + a\hat{\mu}) \\ &\quad - U_\rho^\dagger(x - a\hat{\rho}) U_\mu(x - a\hat{\rho}) U_\rho(x - a\hat{\rho} + a\hat{\mu})) \end{aligned} \quad (3.23)$$

$$\begin{aligned} \delta_\rho^{(2)} U_\mu(x) &\equiv \frac{1}{a^2} (U_\rho(x + a\hat{\rho}) U_\rho^\dagger(x + a\hat{\mu}) \\ &\quad - 2U_\mu(x) \\ &\quad + U_\rho^\dagger(x - a\hat{\rho}) U_\mu(x - a\hat{\rho}) U_\rho(x - a\hat{\rho} + a\hat{\mu})) \end{aligned} \quad (3.24)$$

With this we can define the smearing operator;

$$\mathcal{F}_\mu = \prod_{\rho \neq \mu} \left( 1 + \frac{a^2 \delta_\rho^{(2)}}{4} \right) \quad (3.25)$$

HISQ uses two different smeared gauge fields defined by;

$$X_\mu(x) \equiv \mathcal{U} \mathcal{F}_\mu U_\mu(x) \quad (3.26)$$

$$W_\mu(x) \equiv \left( \mathcal{F}_\mu - \sum_{\rho \neq \mu} \frac{a^2 (\delta_\rho)^2}{2} \right) \mathcal{U} \mathcal{F}_\mu U_\mu(x) \quad (3.27)$$

where  $\mathcal{U}$  is a re-unitarization operator. The HISQ action can then be written as:

$$S_{\text{HISQ}} = \sum_x \bar{\psi}(x) \left( \gamma \cdot \left( \nabla_\mu(W) - \frac{a^2}{6}(1 + \epsilon_{\text{Naik}}) \nabla_\mu^3(X) \right) + m \right) \psi(x) \quad (3.28)$$

Where  $\nabla_\mu(Z)$  is the covariant derivative (3.8) with gauge links repaced with  $Z$ . This action in fact not only removes tree level interactions like fig. 3.1, but also all taste mixing interactions at 1-loop. The  $\nabla_\mu^3$  term is introduced to remove "lattice artifacts", i.e. it reduces the size of  $\mathcal{O}(a)$  terms in the  $a \rightarrow 0$  limit of the action. In the same spirit,  $\epsilon_{\text{Naik}}$  is fixed according to the constraint

$$\lim_{\underline{p} \rightarrow 0} \frac{E^2(\underline{p}) - m^2}{\underline{p}^2} = 1 \quad (3.29)$$

where  $E(\underline{p})$  obeys the dispersion relation from HISQ. The motivation for the specific smearing of the gauge fields (3.27), and more details on HISQ in general, are given in [14].



# Lattice Calculations

---

## 4.1 Correlation Functions from Lattice Simulations

A typical quantity that is computed on the lattice is a meson correlation function, i.e. when  $\mathcal{O} = \Phi(x)\Phi^\dagger(y)$  and  $\Phi$  is a meson creation operator. This is a good working example for showing the steps in a lattice calculation.

A creation operator for a meson in this context can be any operator containing the same quantum numbers as the meson one is trying to create. For example, the neutral  $B$  meson is a pseudoscalar charged with a  $d$  and  $\bar{b}$  quark, so a suitable operator is  $\Phi(x) = \bar{b}(x)\gamma_5 d(x)$ . The path integral can then be written as

$$C(x, y) = \int \mathcal{D}\psi \mathcal{D}\bar{\psi} \mathcal{D}U \left( \bar{b}(x)\gamma_5 d(x) \bar{d}(y)\gamma_5 b(y) \right) e^{-S_G[U] - \sum_{w,z} \bar{\psi}(w)M(w,z)[U]\psi(z)} \quad (4.1)$$

where we have now broken the action up into a gauge part  $S_G[U]$ , and a fermion part.  $M(x, y)[U]$  is the Dirac operator, and can be seen as a matrix in lattice site, flavor, color and spin.  $\psi$  is a vector of quark flavours.

The integral over fermions can be preformed analytically, since the fermion fields are Grassman valued. In our example, the result is [30],

$$C(x, y) = \int \mathcal{D}U \text{Tr} \left[ M_b^{-1}(y, x)[U] \gamma_5 M_d^{-1}(x, y)[U] \gamma_5 \right] e^{-S_G[U] \det(M[U])} \quad (4.2)$$

The quantities  $M_f^{-1}(x, y)[U]$  are propagators of a quark of flavour  $f$  on a fixed gauge background  $U$ . The integration over gauge fields is generally carried out by an importance sampling method. A finite *ensemble* of gauge configurations  $\{U_i\}$  is generated by a Monte Carlo Markov chain (MCMC), where the probability of a gauge configuration  $U_j$  being added to the ensemble is proportional to

$$e^{-S_G[U_j] \det(M[U])} \quad (4.3)$$

See [11] ch. 7 for examples of such algorithms. In the case of our work, we use ensembles generated by the MILC collaboration [5].

Once the ensemble is created, the path integral can be approximated by simply

$$C(x, y) \simeq \frac{1}{N} \sum_i \text{Tr} [ M_b^{-1}(y, x)[U_i]\gamma_5 M_d^{-1}(x, y)[U_i]\gamma_5 ] \quad (4.4)$$

where  $N$  is the size of the ensemble. The calculation of the correlation function then is split into 3 steps:

1. Generate an ensemble of Gauge configurations  $\{U_i\}$  by MCMC.
2. Compute quark propagators  $M_f^{-1}(x, y)[U]$  on each Gauge configuration. This requires inverting the matrix  $M$  each time, this is typically done by conjugate gradient method.
3. Construct trace as in (4.4), and average over the ensemble.

We now turn to the issue of choosing lattice actions.

#### 4.1.1 Path Integral

#### 4.1.2 Dirac Operator Inversion

#### 4.1.3 Random Wall Sources

The full set of spin-mixing matrices can be labelled according to

$$\gamma_n = \prod_{\mu} (\gamma_{\mu})^{n_{\mu}} \quad n_{\mu} = \mathbb{Z}_2 \quad (4.5)$$

There are 16 such matrices representing corners of the hypercube. As  $\gamma_{\mu}^2 = 1$ , one can also use a general site vector  $x_{\mu}$  to label the matrix, then  $\gamma_x = \gamma_n$  where  $n_{\mu} = x_{\mu} \bmod 2$ . One can show that for any  $x$ ;  $\gamma_x^{\dagger} \gamma_x = 1$ .

Naive quarks  $\psi(x)$  can be transformed into staggered quarks  $\chi(x)$  via  $\psi(x) = \gamma_x \chi(x)$ . Then, Naive quark propagators (inverse Dirac operators) become

$$G_{\psi}(x, y) = \gamma_x \gamma_y^{\dagger} G_{\chi}(x, y) \quad (4.6)$$



By conjugating both sides and using  $\gamma_5$ -hermiticity  $G_\psi^\dagger(y, x) = \gamma_5 G_\psi(y, x) \gamma_5$  it can be shown that

$$G_\psi(x, y) = \phi_5(x) \phi_5(y) G_\psi^\dagger(y, x) \quad (4.7)$$

where  $\phi_5(x) = (-1)^{\sum_\mu x_\mu}$ .

## 2pt correlation functions

We will break down the correlation function to see what quantities must be computed by the simulation. Consider the generic 2-point correlator:

$$C(x, y) = \langle \Phi_X^\dagger(x) \Phi_Y(y) \rangle_{\psi, U} \quad , \quad \Phi_X(x) = \frac{1}{4} \bar{\psi}_a(x) \gamma_X \psi_b(x) \quad (4.8)$$

$$= \frac{1}{16} \langle tr_{c,s} \gamma_X G_{a,\psi}(x, y) \gamma_Y G_{b,\psi}(y, x) \rangle_U \quad (4.9)$$

$$= \frac{1}{16} tr_s \left( \gamma_x^\dagger \gamma_X \gamma_x \gamma_y^\dagger \gamma_Y \gamma_y \right) \langle tr_c (G_{a,\chi}(x, y) G_{b,\chi}(y, x)) \rangle_U \quad (4.10)$$

$tr_s$  is a trace over spin and  $tr_c$  is over colour. To deal with the spin trace, define the family of phases  $\{\phi_X(x)\}$  according to

$$\gamma_x^\dagger \gamma_X \gamma_x = \phi_X(x) \gamma_X \quad (4.11)$$

for example, if  $X = 5$ , then  $\gamma_x^\dagger \gamma_5 \gamma_x = (-1)^{\sum_\mu x_\mu} \gamma_x^\dagger \gamma_x \gamma_5 = \phi_5(x) \gamma_5$ . The map from  $X$  to  $\phi_X$  is structure preserving, i.e. if  $\gamma_X = \gamma_A \gamma_B$ , then  $\phi_X(x) = \phi_A(x) \phi_B(x)$ . The spin trace becomes  $\phi_X(x) \phi_Y(y) tr_s (\gamma_X \gamma_Y)$ . The will vanish unless  $Y = X$ , as one would expect physically for the correlation function. We end up with

$$C(x, y) = \frac{1}{4} \phi_X(x) \phi_X(y) \langle tr_c G_{a,\chi}(x, y) G_{b,\chi}(y, x) \rangle_U \quad (4.12)$$

It is useful in the simulation to replace  $G_{b,\chi}(y, x)$  with it's conjugate via (4.7), resulting in

$$C(x, y) = \frac{1}{4} \phi_{5X}(x) \phi_{5X}(y) \langle tr_c G_{a,\chi}(x, y) G_{b,\chi}^\dagger(y, x) \rangle_U \quad (4.13)$$

where  $\phi_{5X}(x) = \phi_5(x) \phi_X(x)$ . To obtain the correlation function of a meson in an eigenstate with momentum  $\underline{p}$ , the above must be replaced with

$$C_{\underline{p}}(t_0, t) = \frac{1}{L^3} \sum_{\underline{x}, \underline{y}} e^{i \underline{p} \cdot (\underline{x} - \underline{y})} C(\underline{x}, t_0; \underline{y}, t) \quad (4.14)$$

$$= \frac{1}{4L^3} \sum_{\underline{x}, \underline{y}} e^{i \underline{p} \cdot (\underline{x} - \underline{y})} \phi_{5X}(x) \phi_{5X}(y) \langle tr_c G_{a,\chi}(x, y) G_{b,\chi}^\dagger(y, x) \rangle_U, \quad (4.15)$$

where it is understood that  $x_0 = t_0$  and  $y_0 = t$ . In order to evaluate this function, the simulation must perform inversions to create  $G_{a/b,\chi}(x, y)$  for each  $x$  and  $y$ , so  $2 \cdot \text{Vol}^2$  operations. This is prohibitively expensive. The number of inversions can be reduced using *random wall sources*. Define

$$P_{a,\underline{p},X}^{t_0}(y) \equiv \frac{1}{\sqrt{L^3}} \sum_{\underline{x}} e^{i\underline{p} \cdot (\underline{x} - \underline{y})} \phi_{5X}(\underline{x}, t_0) \xi(\underline{x}) G_{a,\chi}(\underline{x}, t_0; y), \quad (4.16)$$

where  $\xi(\underline{x})$  is a random field of colour vectors, varying with  $U$ . This has the property

$$\langle f(\underline{x}, \underline{x}') \xi^*(\underline{x}') \xi(\underline{x}) \rangle_U = \delta_{\underline{x}, \underline{y}} \langle f(\underline{x}, \underline{y}) \rangle_U. \quad (4.17)$$

Using this property it can be shown that the correlator can be build instead according to

$$C(\underline{x}, t_0; \underline{y}, t) \simeq \frac{1}{4} \sum_{\underline{y}} \phi_{5X}(y) \langle \text{tr}_c P_{a,\underline{p},X}^{t_0}(\underline{y}, t) P_{b,0,1}^{t_0,\dagger}(\underline{y}, t) \rangle_U \quad (4.18)$$

Now all the simulation has to do is compute  $P_{a/b}^{t_0}(y)$  for general  $y$ , so  $2 \cdot \text{Vol}$  operations, a reduction by a factor of  $\text{Vol}$ .

In the MILC code, "sources" are first created (the fields  $\phi_{5X}(\underline{x}, t_0) \xi(\underline{x})$ ), then the objects  $P^{t_0}(y)$  (referred to as "propagators") are generated from them. Any extra factors dependant on  $y$  (this is useful for "smeared" propagators, see ?) can be multiplied in. The resulting object  $f(y) \cdot P^{t_0}(y)$  is referred to as a "quark". Finally, two of these quarks can be "tied together" according to (4.18), to produce correlation functions. The sources are chosen to be on some single timeslice  $t_0$ , resulting in a value for  $C(t_0, t)$  at each  $t$ .

The above discussion can be generalized to 3-(or  $N$ -)point correlation functions using *extended sources*. Consider a 3-pt correlator encoding the form-factors of a semileptonic decay from meson  $X$  to meson  $Z$ , via a current  $J$ . We start by evaluating

$$\begin{aligned} C(x, y, z) &= \langle \Phi_X^\dagger(x) J(y) \Phi_Z(z) \rangle_{\psi, U} \quad , \quad \Phi_X(x) = \frac{1}{4} \bar{\psi}_b(x) \gamma_X \psi_s(x) \\ J(y) &= \bar{\psi}_b(y) \gamma_J \psi_a(y) \\ \Phi_Z(z) &= \frac{1}{4} \bar{\psi}_a(z) \gamma_Z \psi_s(z) \end{aligned} \quad (4.19)$$

in the same way as before:

$$C(x, y, z) = \frac{1}{16} \text{tr}_s \left( \gamma_x^\dagger \gamma_X \gamma_x \gamma_y^\dagger \gamma_J \gamma_y \gamma_z^\dagger \gamma_Z \gamma_z \right) \langle \text{tr}_c G_{b,\chi}(x, y) G_{a,\chi}(y, z) G_{s,\chi}(z, x) \rangle_U \quad (4.20)$$

$$= \frac{1}{4} \phi_{5X}(x) \phi_J(y) \phi_{5Z}(z) \langle \text{tr}_c G_{b,\chi}(x, y) G_{a,\chi}(y, z) G_{s,\chi}^\dagger(z, x) \rangle_U \quad (4.21)$$

We have assumed that  $\text{tr}_s \gamma_X \gamma_J \gamma_Z = 4$ , requiring that each gamma matrix in this combination has a partner and therefore cancels. In any other situation the trace would vanish. For example, if the current is a temporal vector  $J = 0$ , and the two mesons represent pseudoscalars, one of the meson operators must have a  $\gamma_0$ , i.e. one could choose  $\gamma_X = \gamma_0 \gamma_5$ ,  $\gamma_Z = \gamma_5$ . **why is it ok to have a non-goldstone for  $X$ ?**

Putting  $X$  into an eigenstate of zero momentum, and  $Y$  into an eigenstate of momentum  $\underline{p}$ , we get

$$C_{\underline{p}}(t_0, t, T) = \frac{1}{4L^3} \sum_{\underline{x}, \underline{y}, \underline{z}} e^{i\underline{p} \cdot (\underline{y} - \underline{z})} \phi_{5X}(x) \phi_J(y) \phi_{5Z}(z) \langle \text{tr}_c G_{b,\chi}(\underline{x}, t_0; \underline{y}, t) G_{a,\chi}(\underline{y}, t, \underline{z}, T) G_{s,\chi}^\dagger(\underline{z}, T; \underline{x}, t_0) \rangle_U \quad (4.22)$$

This can be built by first creating propagators for the  $b$  and  $s$  quarks:  $P_{b,0,X}^{t_0}(y), P_{s,0,1}^{t_0}(z)$ . Then, build the  $a$  propagator using an extended source, i.e.:

$$P_{a,p,ext}^T(y) = \sum_{\underline{z}} P_{s,0,1}^{t_0}(\underline{z}, T) \phi_{5Z}(\underline{z}, T) G_{a,\chi}(\underline{z}, T; y) \quad (4.23)$$

Then, by plugging  $P_{b,0,X}^{t_0}(y)$  and  $P_{a,p,ext}^T(y)$  into the MILC tie-together defined by (4.18), one ends up evaluating (4.22).

## 4.2 Analysis of Correlation Functions

### 4.2.1 Non-Linear Regression

Once a correlation function like the in ?? has been computed, we can extract physics from it, namely the mass and decay constant of the meson we are studying. In practice the meson creation operators defined above are fourier transformed

$$\Phi(\underline{k}, t) = \sum_{\underline{x}} e^{-i\underline{k} \cdot \underline{x}} \Phi(\underline{x}, t) \quad (4.24)$$

which serves to change (4.4) into

$$C_{\underline{k}}(t) = \frac{1}{N} \sum_i \sum_{\underline{x}, \underline{y}} e^{-i\underline{k} \cdot (\underline{x} - \underline{y})} \text{Tr} [ M_b^{-1}(\underline{y}, t; \underline{x}, 0) [U_i] \gamma_5 M_d^{-1}(\underline{x}, 0; \underline{y}, t) [U_i] \gamma_5 ] \quad (4.25)$$

(4.25) is computed for many  $t$  values with a lattice calculation following the principles detailed above. One performs a least-squares fit of this to a theoretically motivated function of  $t$ . To derive such a function, first construct a complete set of momentum  $\underline{k}$  states with quantum numbers matching the meson:

$$1 = \sum_{n=0} \frac{1}{2E_n^r} |\lambda_n\rangle \langle \lambda_n|. \quad (4.26)$$

Where  $E_n^r = \sqrt{M_n^2 + \underline{k}^2}$  are the relativistic energies of each state. Inserting this into the correlation function, and moving from the Heisenberg to Schroedinger picture;

$$\begin{aligned} C_{\underline{k}}(t) &= \sum_{n=0} \frac{1}{2E_n^r} \langle 0 | e^{Ht} \Phi(\underline{k}, 0) e^{-Ht} | \lambda_n \rangle \langle \lambda_n | \Phi^\dagger(\underline{k}, 0) | 0 \rangle \\ &= \sum_{n=0} \left( \frac{\langle 0 | \Phi(\underline{k}, 0) | \lambda_n \rangle}{\sqrt{2E_n^r}} \right) \left( \frac{\langle \lambda_n | \Phi^\dagger(\underline{k}, 0) | 0 \rangle}{\sqrt{2E_n^r}} \right) e^{-E_n^l t} \\ &\equiv \sum_{n=0} |a_n|^2 e^{-E_n^l t}. \end{aligned} \quad (4.27)$$

The fit results in a determination of the parameters  $a_n$ , and  $E_n^l$ . Since the lowest energies dominate the function at late times, one can afford to truncate the sum over  $n$  to some tractable range, in our case  $n \in [1, 6]$ . We interpret  $|\lambda_0\rangle$  to be the ground state of the meson we are studying. The exponential decays mean the fit function is dominated by the ground state at large  $t$ , and subsequent excited states become less important as  $E_n^l$  increases. Hence by only including  $C_{\underline{k}}(t)$  at suitably large  $t$  values, we can afford to truncate the sum in  $n$ . In our fits we chose  $n = 6$ .

We maintain a distinction between  $E^l$  and  $E^r$ , since for example in simulations involving NRQCD quarks these differ. If this is not an issue, as is the case with HISQ, one can compute the correlation function at zero momentum  $C_0(t)$ , then fit it to find the parameter  $E_0^l$ , which will equal the meson's mass  $M$ . Noting the definition of a meson decay constant  $f$ :  $\langle 0 | J_0 | \text{Meson}(\underline{k} = 0) \rangle = Mf$ , where  $J_0$  is a temporal current with the same quantum numbers as the meson, we can see that the fit parameters  $a_n$  at zero momentum are related to the meson's decay constant

via

$$f = \sqrt{\frac{2}{M}} a_0 \quad (4.28)$$

Hence the fit can also be used to extract decay constants.

The above discussion can be straightforwardly generalized to 3-point correlation functions, from which we are able to extract quantities like the hadronic transition amplitudes  $H_\mu = \langle M_{q_1 \bar{q}_3} | J_\mu^{q_1 \bar{q}_2} | M_{q_2 \bar{q}_2} \rangle$  from sec. ???. Specifically the quantity we require in order to deduce the  $B_s \rightarrow D_s l \nu$  form factors is  $\langle D_s | V_\mu | B_s \rangle$ , where  $V_\mu = \bar{c} \gamma_\mu b$ .

The generalization of the above for 3pt functions is summarized here:

$$C_3(t, T) = \int \mathcal{D}\psi \mathcal{D}\bar{\psi} \mathcal{D}U \left( \Phi_{D_s}(\underline{0}, 0) V_\mu(-\underline{p}, t) \Phi_{B_s}^\dagger(\underline{p}, T) \right) e^{-S[\psi, \bar{\psi}, U]} \quad (4.29)$$

$$\simeq \frac{1}{N} \sum_i \sum_{\underline{x}, \underline{y}, \underline{z}} e^{-i \underline{p} \cdot (\underline{y} - \underline{z})} \text{Tr} \left[ M_b^{-1}(\underline{x}, 0; \underline{y}, t) [U_i] \gamma_\mu M_c^{-1}(\underline{y}, t; \underline{z}, T) [U_i] \gamma_5 \gamma_5 M_s^{-1\dagger}(\underline{z}, T; \underline{x}, 0) [U_i] \right] \quad (4.30)$$

$$= \sum_{n, m} \left( \frac{\langle 0 | \Phi_{D_s} | \lambda_n \rangle}{\sqrt{2E_n^r}} \right) \left( \frac{\langle \lambda_n | V_\mu | \lambda_m \rangle}{2\sqrt{E_n^r E_m^r}} \right) \left( \frac{\langle \lambda_m | \Phi_{B_s}^\dagger | 0 \rangle}{\sqrt{2E_n^r}} \right) e^{-E_m^l(T-t)} e^{-E_n^l t} \quad (4.31)$$

$$\equiv \sum_{n, m} a_{D_s, n} V_{nm} a_{B_s, m}^* e^{-E_m^l(T-t)} e^{-E_n^l t}.$$

$C(t, T)$  is computed at different values of  $t$  and  $T$ , then a least-squares fit is performed to the fit function (4.32).  $a_n$  will vanish for states  $|\lambda_n\rangle$  which have different quantum numbers to  $\Phi_{B_s}$ , and similarly for  $b_m$  and  $\Phi_{D_s}$ . Non-zero  $a_n$ 's will match the analogous parameters extracted from fitting a 2pt function  $\langle \Phi_{B_s}^\dagger \Phi_{B_s} \rangle$ , similarly for  $b_n$ 's and  $\Phi_{D_s}$ . This carries on to the energies,  $\{E_n^l\}$  is the spectrum for the  $D_s$  meson, and  $\{E_m^l\}$  is the spectrum for the  $B_s$ . Therefore, we compute and fit the appropriate 2pt functions to deduce the parameters  $\{a_n\}, \{b_m\}, \{E_n^l\}$ . Then, fitting  $C_3(t, T)$  results in an accurate determination of the remaining free parameters,  $V_{nm}$ . This set contains the quantity we need, recognising that:

$$V_{00} = \frac{\langle D_s | V_\mu | B_s \rangle}{2\sqrt{E^{B_s} E^{D_s}}} \quad (4.32)$$

2-point correlation functions are then fitted as in sec. ???. The fit function we

use is modified a little from (4.27), we use:

$$C^{\alpha\beta}(t) = \sum_n a_n^{\alpha*} a_n^\beta (e^{-E_n^l t} - s e^{-E_n^l (T-t)}) + \sum_n a_n^{\prime\alpha*} a_n^{\prime\beta} (-1)^t (e^{-E_n^{\prime l} t} - s e^{-E_n^{\prime l} (T-t)}) \quad (4.33)$$

Firstly, the parameters  $\{a_n\}$  must vary between source and sink to account for the different operators. Secondly, the periodicity of the lattice in the time direction means an extra exponential term is required, but not in the case of the  $B_s$  since NRQCD quarks do not experience the periodicity of the lattice. Hence  $s$  is set to 0 for the  $B_s$  correlator and 1 for the  $D_s$ .  $T$  is the time extent of the lattice. The second term is to account for the so-called "oscillating state", which is in fact the  $\zeta = (1, 0, 0, 0)$  doubler fermion appearing due to the doubling in the HISQ action (see sec. 3.15). No other doublers contribute, since  $\Phi_{\underline{k}}$  has a 3-momentum fixed at  $\underline{k}$ , which we always take to be small relative to  $\pi/a$ , hence does not couple to the states at  $k \sim (0, \pi/a, 0, 0)$ ,  $k \sim (0, 0, \pi/a, 0)$  etc. However,  $\Phi_{\underline{k}}$  can couple to arbitrarily high energy states, so the  $k \sim (\pi/a, 0, 0, 0)$  doubler contributes. The second term in (4.33) is justified by performing the doubling operation  $\mathcal{B}_0$  defined in (4.27), the quark fields in  $\Phi_{\underline{k}}$  which obey the HISQ action. See appendix G of [14] for details.

We use the *CorrFitter* package [16] for performing Bayesian least-squares fitting to the correlation functions. The package employs the trust region method of least-squares fitting. The fits require priors for each of the fit parameters. The "amplitude" parameters  $a_{n,B_s/D_s}^\alpha$  are given priors of 0.1(1.0), thus inserting only the assumption that they are of  $\mathcal{O}(1)$ . The ground state energies are given priors motivated by the meson masses, and excited state energies are given loose, evenly spaced priors with 600MeV between each level.

2-point correlation functions for  $B_s$  and  $D_s$  are fit to (4.33), resulting in  $a_{n,B_s/D_s}^\alpha, E_{n,B_s/D_s}^l$ . Since the HISQ action is fully relativistic,  $E_{0,D_s}^l$  at  $\underline{k} = 0$  can be interpreted as the  $D_s$  meson mass. The same cannot be done for the  $B_s$ . The decay constants for  $B_s$  and  $D_s$  can be deduced from  $a_{0,B_s}^0$  and  $a_{0,D_s}^0$ , since  $\Phi_{B_s,D_s}^0$  are also temporal axial currents. This is a good avenue for consistency checks, we compared  $M_{D,s}, f_{D_s}$  and  $f_{B_s}$  to those computed in [9], [26] amongst others, and found them to be consistent (modulo small shifts we can reasonably expect due to differing choices of bare quark masses).

We now discuss fitting the 3-point correlation functions. The same considerations as those that went into (4.33) lead us to our 3-point fit function:

$$\begin{aligned}
C_3^{\alpha\beta}(t, T) = & \sum_{k,m} (a_{k,D_s}^\alpha V_{km}^{nn} a_{m,B_s}^{*\beta} e^{-E_m^l t} e^{-E_k^l(T-t)} \\
& + a_{k,D_s}^\alpha V_{km}^{no} a_{m,B_s}^{*\beta} e^{-E_m^l t} e^{-E_k^l(T-t)} \\
& + a_{k,D_s}'^\alpha V_{km}^{on} a_{m,B_s}^{*\beta} e^{-E_m^l t} e^{-E_k^l(T-t)} \\
& + a_{k,D_s}'^\alpha V_{km}^{oo} a_{m,B_s}^{*\beta} e^{-E_m^l t} e^{-E_k^l(T-t)}) \quad (4.34)
\end{aligned}$$

The 2-point and 3-point correlators are fit simultaneously, according to fit functions (4.33) and (4.34). The parameters involved in the 2pt fits are mostly fixed by the data in the 2pt correlation functions, so the fit can use most of the data in the 3pt correlation functions to determine the transition amplitudes  $V_{km}^{ab}$ . This is carried out for each  $B_s$  and  $D_s$  smearing, each direction  $\mu$  and each current correction  $i$  of the vector current  $V_\mu^{(i)}$ .

In this large 2pt/3pt fit, there is a huge  $\chi^2$  manifold with many local minima, and it is crucial to impose strong priors in order to ensure the fit finds the true minimum. Priors for ground state 2-point amplitudes and energies  $a_{0,B_s/D_s}^\alpha, E_{0,B_s/D_s}^l$  are taken to be the results from individual fits of the 2-point functions, with the errors expanded by a factor of 2. The excited state amplitudes and energies are given the same priors as in the 2-point fits. The transition amplitudes  $V_{km}^{ab}$  are given the prior 0.1(1.0), assuming it to be  $\mathcal{O}(1)$ .

Finally, we end up with the sought-after parameters  $V_{00}^{nn}$  representing  $V_\mu^{(i)}$ , via the relation

$$\langle D_s | V_\mu^{(i)} | B_s \rangle = 2\sqrt{M^{B_s} E^{D_s}} V_{00}^{nn} |_{V=V_\mu^{(i)} \text{ in simulation}} \quad (4.35)$$

We have asserted the ground state of  $B_s$  to be its mass, but not the  $D_s$ , as we give  $D_s$  spacial momenta in the calculation (to be expanded on in the next section). Then, the full vector currents  $\langle D_s | V_\mu^{(i)} | B_s \rangle$  can be built from a linear combination of these according to ??.

### 4.2.2 Signal/Noise Ratio

One of the main obstacles in our calculation is the *signal degradation* of correlation functions computed on the lattice.

A random variable  $x$  has mean and standard deviation

$$\hat{x} = \langle x \rangle \quad (4.36)$$

$$\sigma^2 = \frac{1}{N}(\langle x^2 \rangle - \langle x \rangle^2), \quad (4.37)$$

where  $N$  is the size of the sample. So the (square of) the signal/noise ratio is

$$\frac{\hat{x}^2}{\sigma^2} = N \left( \frac{\langle x^2 \rangle}{\langle x \rangle^2} - 1 \right)^{-1}. \quad (4.38)$$

Consider 2 point correlators where  $x = \Phi^\dagger(t)\Phi(0)$ , where  $\Phi$  is a meson operator with zero spacial momentum.

$\langle x^2 \rangle$  and  $\langle x \rangle$  can be written as

$$\langle x \rangle = \sum_k \frac{1}{2E_n} \langle 0 | \Phi^\dagger(t) | \lambda_n \rangle \langle \lambda_n | \Phi(0) | 0 \rangle e^{-E_n t} \simeq_{t \rightarrow \infty} e^{-E_0 t} \quad (4.39)$$

$$\langle x^2 \rangle = \sum_n \frac{1}{2E_n} \langle 0 | \Phi^{\dagger 2}(t) | \lambda_n \rangle \langle \lambda_n | \Phi^2(0) | 0 \rangle e^{-E_n t} \simeq_{t \rightarrow \infty} e^{-E'_0 t} \quad (4.40)$$

where we have assumed the ratio of matrix elements and energies are  $\mathcal{O}(1)$ . The two ground state energies  $E_0$  and  $E'_0$  need not be the same, since the lowest states for which  $\langle \lambda_n | \Phi(0) | 0 \rangle \neq 0$  and  $\langle \lambda_n | \Phi^2(0) | 0 \rangle \neq 0$  may differ.

The operator  $\Phi^2$  will contain two quark and two antiquark operators, connected by some matrices in spin space.  $\Phi^2$  can create a combination of all possible 2 meson states where the mesons are made of the available quark species, and quantum numbers. For example, If  $\Phi$  is a pion,  $\Phi^2$  is a 2 pion state, and  $E'_0 = 2m_\pi$ . If  $\Phi$  is a  $D_s$  meson, then  $E'_0 = m_{\tilde{\pi}} + m_{\eta_c}$  ( $\tilde{\pi}$  is a pseudoscalar  $s\bar{s}$  state).

Define  $\mu_0 = E'_0/2$ . Then

$$\frac{\hat{x}^2}{\sigma^2} \simeq N \left( e^{-2(\mu_0 - m_\Phi)t} - 1 \right)^{-1} \quad (4.41)$$

In the case of pions,  $\mu_0 = m_\Phi$ , the ratio becomes simply  $\sim N$ . For mesons heavier than the pion,  $\mu_0 < m_\Phi$ , so at large times  $e^{-2(\mu_0 - m_\Phi)t} \gg 1$ , and upon taylor expanding the inverse of this phase we arrive at

$$\frac{\hat{x}}{\sigma} \simeq \sqrt{N} e^{-(m_\Phi - \mu_0)t} \quad (4.42)$$

From this we see there are 3 variables which effect the quality of the signal:



1. The size of the sample  $N$ .
2. At large  $t$ , the correlators undergo *signal degradation*, i.e., become dominated by noise.
3. The degree of signal degradation is decided by  $m_\varphi - \mu_0$ . Heavier mesons will tend to experience more signal degradation.

Relevant to our calculation is how giving mesons non-zero spacial momenta  $\underline{p}$  can exaserbate this problem. In this case,  $m_\Phi$  in (4.42) is replaced with  $\sqrt{m_\Phi^2 + \underline{p}^2}$ . As  $\underline{p}$  increases, the signal/noise ratio will degrade more and more and statistics will suffer.

In the  $B_s \rightarrow D_s l \nu$  calculation, to deduce form factors over the whole range of  $q^2$  values, we need to simulate the process with the  $D_s$  having a range of momenta  $0 < |\underline{p}| < 2.32\text{GeV}$ , as discussed in sec. ?? . Correlation functions at the higher end of this range may be too noisy for any meaningful results to be extracted. We are investigating ways of taming this problem, see sec. ?? .

## 4.3 Dealing with Heavy Quarks

### 4.3.1 Heavy HISQ

### 4.3.2 Lattice NRQCD

## 4.4 Renormalization of Currents

Once one has computed a matrix element from a lattice calculation, it needs to be translated into a continuum regularization scheme. Suppose we have some bare operator  $\mathcal{O}_0$ , we expect this to be related to the renormalized operator in  $\overline{MS}$  at scale  $\mu$ ,  $\mathcal{O}^{\overline{MS}}(\mu)$ , via

$$\mathcal{O}^{\overline{MS}}(\mu) = Z^{\overline{MS}}(\mu) \mathcal{O}_0. \quad (4.43)$$

Similarly, in a lattice regularization,

$$\mathcal{O}^{\text{lat}}(1/a) = Z^{\text{lat}}(1/a) \mathcal{O}_0. \quad (4.44)$$

Hence we expect a multiplicative factor between the lattice matrix elements, and the continuum  $\overline{MS}$  ones:

$$\langle \mathcal{O} \rangle^{\overline{MS}} = Z(\mu, 1/a) \langle \mathcal{O} \rangle^{\text{lat}} \quad (4.45)$$

where  $\mathcal{Z}(\mu, 1/a) = Z^{\overline{MS}}(\mu)/Z^{\text{lat}}(1/a)$ . These "matching factors"  $\mathcal{Z}$  can be deduced by equating observables calculated in both lattice QCD and continuum (appropriately regularized) QCD, producing equations which can be solved for  $\mathcal{Z}$ . The lattice side of the calculation can be done either through lattice perturbation theory ("perturbative matching"), or through a simulation ("non-perturbative matching").

It is a well-known result that conserved (or partially conserved) currents do not receive any renormalization in any scheme, i.e.  $Z^{\text{any}} = 1$  ("absolutely normalized").

In principle this is of great help, since the currents we are calculating, namely  $V_\mu$ , are partially conserved, so we are not required to include any matching factors. However in practice, this is complicated by the fact that the conserved current in the lattice theory is often computationally difficult or impossible to compute. For example, in NRQCD, the partially conserved current corresponding to  $SU(N)_V$  is an infinite sum in  $1/m_b$  where  $m_b$  is the bottom mass. The corresponding current in HISQ is also the sum of a large number of operators. This can be interpreted as a mixing in the renormalization:

$$\langle \mathcal{O}_i \rangle^{\overline{MS}} = \mathcal{Z}_{i,j} \langle \mathcal{O}_j \rangle^{\text{lat}} \quad (4.46)$$

In practice, lattice calculations often use only the dominant operators that contribute to the conserved current. Since these will be "close" to the conserved current, one can expect the matching factor to only be a small deviation from unity, and the more sub-dominant operators you add, the overall matching factor should tend towards one.

#### 4.4.1 Non-perturbative Renormalization of HISQ Currents

#### 4.4.2 Matching NRQCD currents to $\overline{MS}$

# List of Figures

1.1	Semileptonic decay at tree level . . . . .	1
1.2	$R(D)/R(D^*)$ determinations from standard model and experiment [18]	5
3.1	Taste mixing at tree level. . . . .	16



# List of Tables



# Bibliography

- [1] Roel Aaij et al. Measurement of the ratio of branching fractions  $\mathcal{B}(\bar{B}^0 \rightarrow D^{*+}\tau^-\bar{\nu}_\tau)/\mathcal{B}(\bar{B}^0 \rightarrow D^{*+}\mu^-\bar{\nu}_\mu)$ . *Phys. Rev. Lett.*, 115(11):111803, 2015. [Erratum: *Phys. Rev. Lett.*115,no.15,159901(2015)].
- [2] Wolfgang Altmannshofer, Peter Stangl, and David M. Straub. Interpreting Hints for Lepton Flavor Universality Violation. 2017.
- [3] S. Aoki et al. Review of lattice results concerning low-energy particle physics. *Eur. Phys. J.*, C77(2):112, 2017.
- [4] Gunnar S. Bali, Bernhard Lang, Bernhard U. Musch, and Andreas Schäfer. Novel quark smearing for hadrons with high momenta in lattice QCD. *Phys. Rev.*, D93(9):094515, 2016.
- [5] A. Bazavov et al. Lattice QCD ensembles with four flavors of highly improved staggered quarks. *Phys. Rev.*, D87(5):054505, 2013.
- [6] Bugra Borasoy. Introduction to Chiral Perturbation Theory. *Springer Proc. Phys.*, 118:1–26, 2008.
- [7] Claude Bourrely, Laurent Lellouch, and Irinel Caprini. Model-independent description of  $b \rightarrow \pi l \nu$  decays and a determination of  $|V_{ub}|$ . *Phys. Rev. D*, 79:013008, Jan 2009.
- [8] Bipasha Chakraborty, C. T. H. Davies, B. Galloway, P. Knecht, J. Koponen, G. C. Donald, R. J. Dowdall, G. P. Lepage, and C. McNeile. High-precision quark masses and qcd coupling from  $n_f = 4$  lattice qcd. *Phys. Rev. D*, 91:054508, Mar 2015.
- [9] B. Colquhoun, C. T. H. Davies, R. J. Dowdall, J. Kettle, J. Koponen, G. P. Lepage, and A. T. Lytle. B-meson decay constants: a more complete picture from full lattice QCD. *Phys. Rev.*, D91(11):114509, 2015.
- [10] Brian Colquhoun, Christine Davies, Jonna Koponen, Andrew Lytle, and Craig McNeile.  $B_c$  decays from highly improved staggered quarks and NRQCD. *PoS, LATTICE2016*:281, 2016.

- [11] Thomas DeGrand and Carleton E. Detar. *Lattice methods for quantum chromodynamics*. 2006.
- [12] R. J. Dowdall et al. The Upsilon spectrum and the determination of the lattice spacing from lattice QCD including charm quarks in the sea. *Phys. Rev.*, D85:054509, 2012.
- [13] Leslie L. Foldy and Siegfried A. Wouthuysen. On the dirac theory of spin 1/2 particles and its non-relativistic limit. *Phys. Rev.*, 78:29–36, Apr 1950.
- [14] E. Follana, Q. Mason, C. Davies, K. Hornbostel, G. P. Lepage, J. Shigemitsu, H. Trotter, and K. Wong. Highly improved staggered quarks on the lattice, with applications to charm physics. *Phys. Rev.*, D75:054502, 2007.
- [15] Christof Gattringer, Meinulf Gockeler, Paul E. L. Rakow, Stefan Schaefer, and Andreas Schaefer. A Comprehensive picture of topological excitations in finite temperature lattice QCD. *Nucl. Phys.*, B618:205–240, 2001.
- [16] G.P.Lepage. Corrfitter, 2012.
- [17] A. Gray, I. Allison, C. T. H. Davies, Emel Dalgic, G. P. Lepage, J. Shigemitsu, and M. Wingate. The Upsilon spectrum and  $m(b)$  from full lattice QCD. *Phys. Rev.*, D72:094507, 2005.
- [18] Heavy Flavour Averaging Group. Rd plane, 2015.
- [19] T. C. Hammant, A. G. Hart, G. M. von Hippel, R. R. Horgan, and C. J. Monahan. Radiative improvement of the lattice nonrelativistic QCD action using the background field method with applications to quarkonium spectroscopy. *Phys. Rev.*, D88(1):014505, 2013. [Erratum: *Phys. Rev.* D92,no.11,119904(2015)].
- [20] Richard J. Hill. The Modern description of semileptonic meson form factors. *eConf*, C060409:027, 2006.
- [21] Karl Jansen. Domain wall fermions and chiral gauge theories. *Phys. Rept.*, 273:1–54, 1996.
- [22] G. P. Lepage. Lattice QCD for novices. In *Strong interactions at low and intermediate energies. Proceedings, 13th Annual Hampton University Graduate Studies, HUGS'98, Newport News, USA, May 26-June 12, 1998*, pages 49–90, 1998.



- [23] G. P. Lepage, B. Clark, C. T. H. Davies, K. Hornbostel, P. B. Mackenzie, C. Morningstar, and H. Trotter. Constrained curve fitting. *Nucl. Phys. Proc. Suppl.*, 106:12–20, 2002. [,12(2001)].
- [24] G. Peter Lepage, Lorenzo Magnea, Charles Nakhleh, Ulrika Magnea, and Kent Hornbostel. Improved nonrelativistic QCD for heavy quark physics. *Phys. Rev.*, D46:4052–4067, 1992.
- [25] Christopher Monahan, Junko Shigemitsu, and Ron Horgan. Matching lattice and continuum axial-vector and vector currents with nonrelativistic QCD and highly improved staggered quarks. *Phys. Rev.*, D87(3):034017, 2013.
- [26] Christopher J Monahan, Heechang Na, Chris M Bouchard, G Peter Lepage, and Junko Shigemitsu.  $B_s \rightarrow D_s \ell \nu$  Form Factors and the Fragmentation Fraction Ratio  $f_s/f_d$ . 2017.
- [27] G. Munster and M. Walzl. Lattice gauge theory: A Short primer. In *Phenomenology of gauge interactions. Proceedings, Summer School, Zuo, Switzerland, August 13-19, 2000*, pages 127–160, 2000.
- [28] Heechang Na, Chris M. Bouchard, G. Peter Lepage, Chris Monahan, and Junko Shigemitsu.  $B \rightarrow D \ell \nu$  form factors at nonzero recoil and extraction of  $|V_{cb}|$ . *Phys. Rev.*, D92(5):054510, 2015. [Erratum: *Phys. Rev.*D93,no.11,119906(2016)].
- [29] R. Narayanan. Tata lectures on overlap fermions. 2011.
- [30] Michael E. Peskin and Daniel V. Schroeder. *An Introduction to quantum field theory*. 1995.
- [31] Jeffrey D. Richman and Patricia R. Burchat. Leptonic and semileptonic decays of charm and bottom hadrons. *Rev. Mod. Phys.*, 67:893–976, 1995.
- [32] Matthew D. Schwartz. *Quantum Field Theory and the Standard Model*. Cambridge University Press, 2014.
- [33] Matthew Wingate.  $|V_{cb}|$  using lattice QCD. In *9th International Workshop on the CKM Unitarity Triangle (CKM2016) Mumbai, India, November 28-December 3, 2016*, 2017.